

## Supporting Information

### **Ultra-stable Mn-based Prussian Blue Compound Effectively Suppresses Jahn-Teller Distortion as Superior Cathode Material for Sodium-ion Batteries**

Xiangyu Ding,<sup>a</sup> Qingbo Zhou,<sup>a</sup> Ziyi Wang,<sup>a</sup> Lei Liu,<sup>a</sup> Yusong Wang,<sup>a, b</sup> Tinglu Song,<sup>c</sup>  
Feng Wu,<sup>a</sup> Hongcai Gao,<sup>a, b, d\*</sup>

<sup>a</sup> School of Materials Science and Engineering, Beijing Institute of Technology, Beijing, 100081, China

<sup>b</sup> Yangtze Delta Region Academy of Beijing Institute of Technology, Jiaxing, 314019, China

<sup>c</sup> Experimental Center of Advanced Materials, School of Materials Science and Engineering, Beijing Institute of Technology, Beijing, 100081, China

<sup>d</sup> Beijing Institute of Technology Chongqing Innovation Center, Chongqing, 401120, China

\*Corresponding author at School of Materials Science and Engineering, Beijing Institute of Technology, Beijing, 100081, China

E-mail address: gaohc@bit.edu.cn (H. Gao)

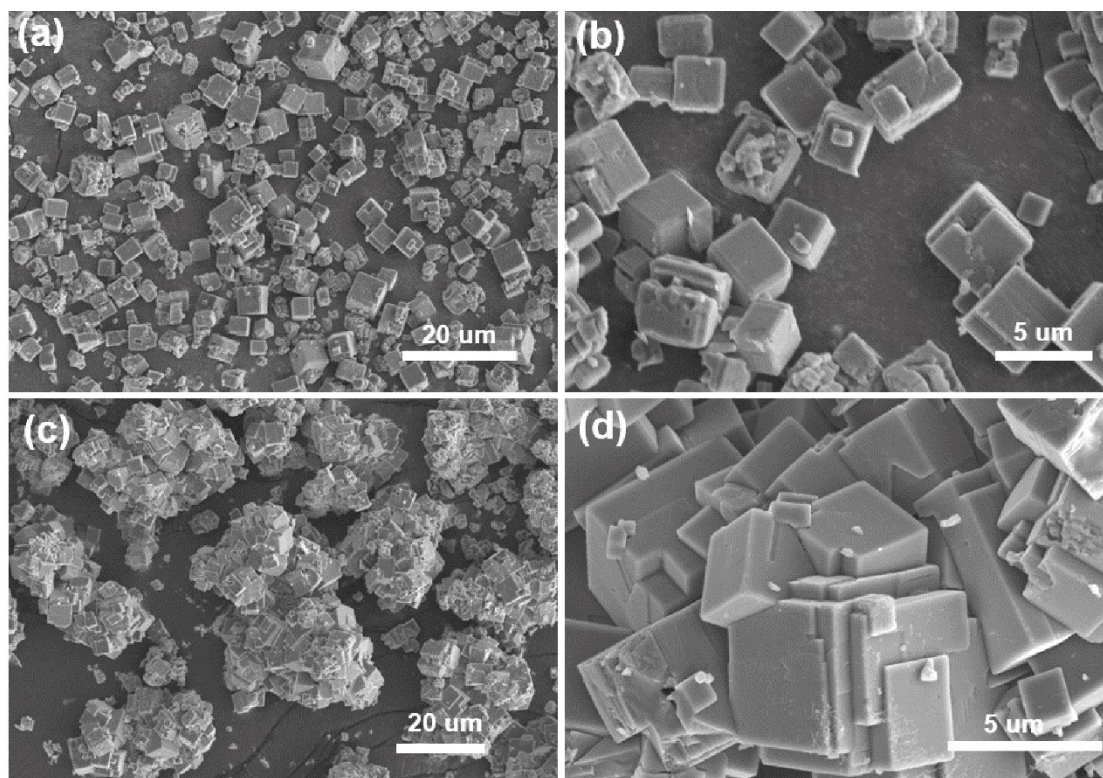


Fig. S1 (a-b) SEM images of the NaMHCF-2 at different magnifications; (c-d) SEM images of the NaMHCF-3 at different magnifications.

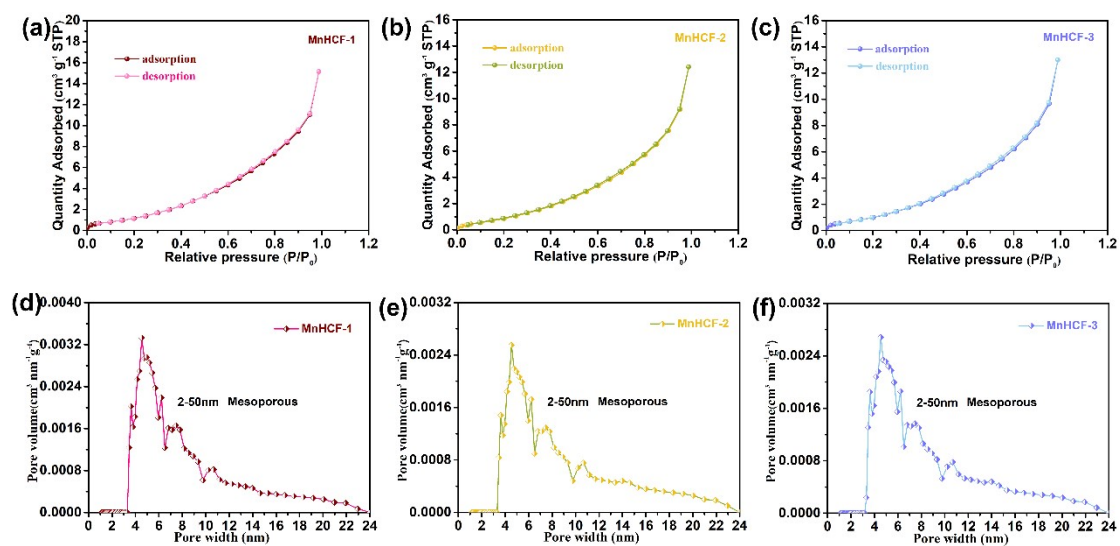


Fig. S2 (a-c)  $N_2$  adsorption-desorption isotherms of MHCF-1, MHCF-2, MHCF-3; (d-f) Pore size distribution of MHCF-1, MHCF-2, MHCF-3.

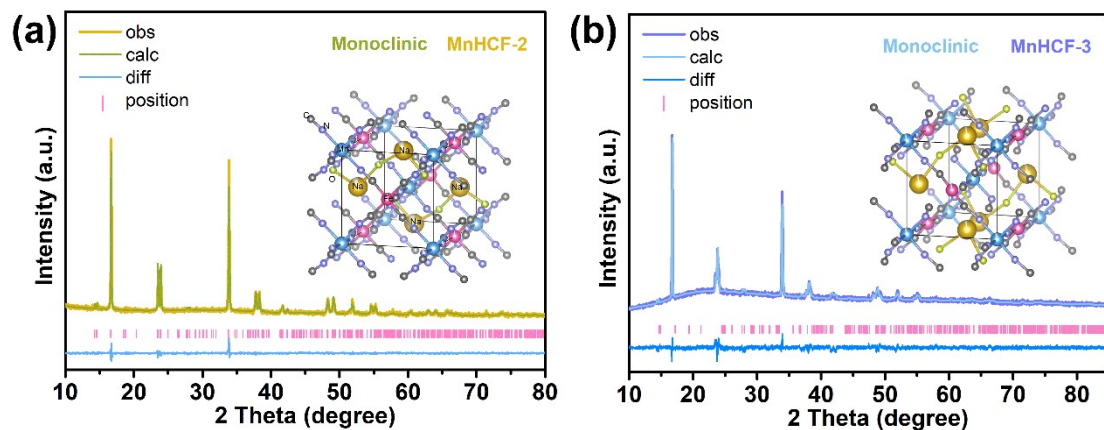


Fig. S3 The Rietveld refinements of the monoclinic phase (a) MnHCF-2; (b) MnHCF-3.

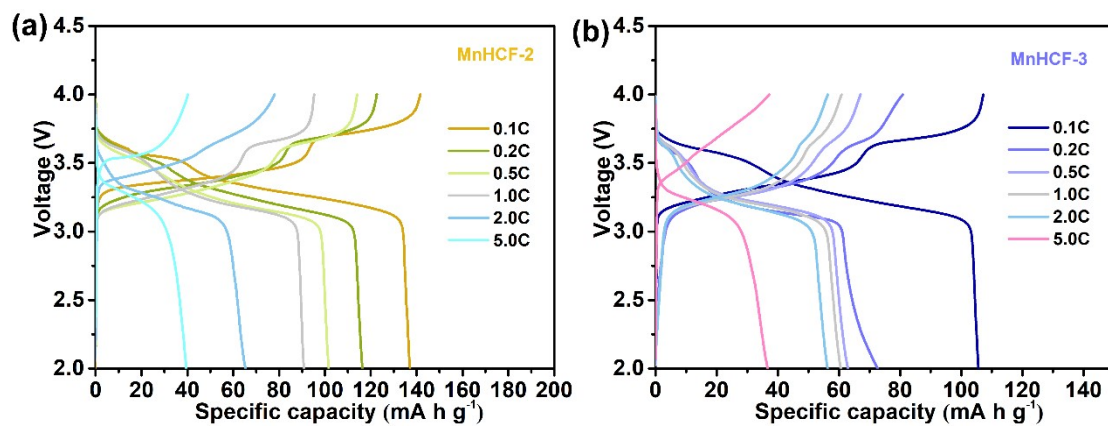


Fig. S4 Charge and discharge curves at different current densities (a) MnHCF-2; (b) MnHCF-3.

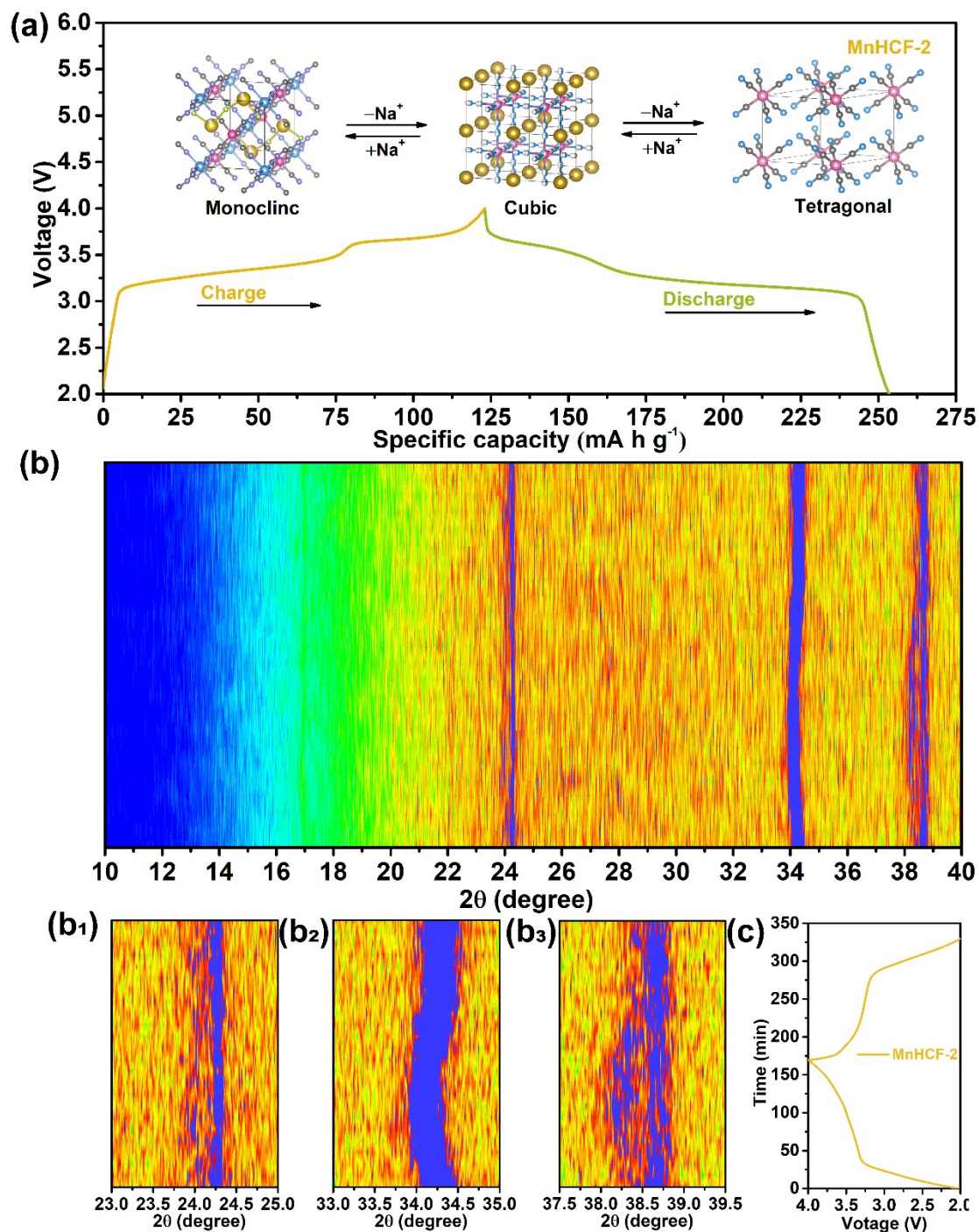


Fig. S5 (a) Galvanostatic charge/discharge voltage curve and schematic illustration of structural phase transformation of MnHCF-2; (b) In situ XRD patterns in intensity contour maps of MnHCF-1; (b<sub>1</sub>-b<sub>3</sub>) A partial enlargement of figure b; (c) the corresponding galvanostatic charge/discharge voltage curves at 0.2 C.

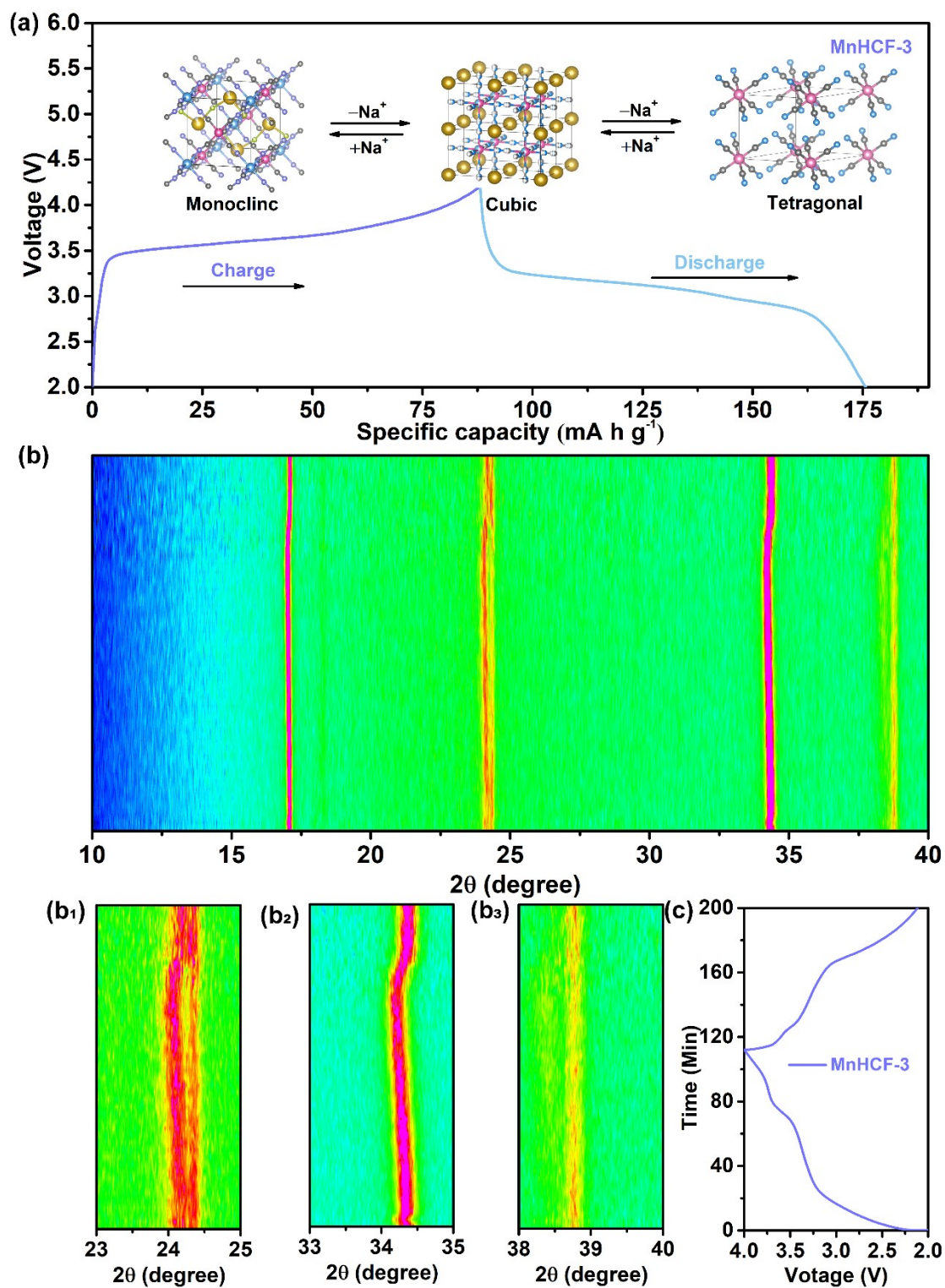


Fig. S6 (a) Galvanostatic charge/discharge voltage curve and schematic illustration of structural phase transformation of MnHCF-3; (b) In situ XRD patterns in intensity contour maps of MnHCF-1; (b<sub>1</sub>-b<sub>3</sub>) A partial enlargement of figure b; (c) the corresponding galvanostatic charge/discharge voltage curves at 0.2 C

Table S1 Structure Parameters of MnHCF-1

Pm/3m Cubic a=b=c=5.25620 Å, $\alpha=\gamma=\beta=90^\circ$				
Atom	x	y	z	Site
Na1	0.00000	0.00000	0.00000	1a
Fe1	0.50000	0.50000	0.50000	1b
Mn1	0.50000	0.50000	0.50000	1b
C1	0.50000	0.08624	0.50000	4m
N1	0.50000	0.08300	0.50000	4m

Table S2 Structure Parameters of MnHCF-2

P21/n Monoclinic a=10.5467 Å, b=7.5016 Å, c=7.4116 Å, $\alpha=\gamma=90^\circ$ , $\beta=91.3770^\circ$				
Atom	x	y	z	Site
Mn	0.50000	0.50000	0.50000	2a
Fe	0.50000	0.00000	1.00000	2d
C1	0.49338	0.18403	0.81012	4e
C2	0.22367	0.51529	0.54315	4e
C3	0.49083	0.16830	0.18496	4e
N1	0.49940	0.30420	0.72200	4e
N2	0.29070	0.49680	0.49710	4e
N3	0.49930	0.29050	0.29500	4e
O1	0.25070	0.21250	0.29150	4e
Na1	0.24880	0.44010	0.04180	4e

Table S3 Structure Parameters of MnHCF-3

P21/n Monoclinic a=10.53440 Å, b=7.53540 Å, c=7.37630 Å, $\alpha=\gamma=90^\circ$ , $\beta=90.4190^\circ$				
Atom	x	y	z	Site
Mn	0.50000	0.50000	0.50000	2a
Fe	0.50000	0.00000	1.00000	2d
C1	0.42618	0.28930	0.78334	4e

C2	0.23710	0.48944	0.52438	4e
C3	0.48944	0.13961	0.16125	4e
N1	0.49896	0.29271	0.70242	4e
N2	0.27207	0.49827	0.51144	4e
N3	0.50322	0.30102	0.29598	4e
O1	0.23007	0.26243	0.29274	4e
Na1	0.28431	0.46595	-0.01155	4e

Table S4 The bulk atomic ratio obtained from ICP-OES and TGA of the samples of MnHCF-1, MnHCF-2, and MnHCF-3.

Quality weight (wt%)	Na	Mn	Fe	□	H <sub>2</sub> O
MnHCF-1	1.217	1	0.862	0.138	1.99
MnHCF-2	1.139	1	0.813	0.187	2.78
MnHCF-3	1.143	1	0.417	0.583	5.68

Table S5 Comparison table of previously reported Mn-based PBA electrodes and this work.

	10 mA g <sup>-1</sup>	25 mA g <sup>-1</sup>	50 mA g <sup>-1</sup>	100 mA g <sup>-1</sup>	References
C-MnHCF		123.8 mAh g <sup>-1</sup>	117.2 mAh g <sup>-1</sup>	110.2 mAh g <sup>-1</sup>	<sup>1</sup>
M-MnHCF		140.0 mAh g <sup>-1</sup>	125.0 mAh g <sup>-1</sup>	110.0 mAh g <sup>-1</sup>	<sup>1</sup>
L-PBM	150 mAh g <sup>-1</sup>		138.0 mAh g <sup>-1</sup>	130.0 mAh g <sup>-1</sup>	<sup>2</sup>
EDTA-NMF		137.0 mAh g <sup>-1</sup>	129.0 mAh g <sup>-1</sup>	119.0 mAh g <sup>-1</sup>	<sup>3</sup>
Na-MnHCF		100.0 mAh g <sup>-1</sup>	70.0 mAh g <sup>-1</sup>	40.0 mAh g <sup>-1</sup>	<sup>4</sup>

NMF HFC	105.0 mAh g <sup>-1</sup>	90.0 mAh g <sup>-1</sup> 1	85.0 mAh g <sup>-1</sup> 1	65.0 mAh g <sup>-1</sup>	<sup>5</sup>
MnHCF-1	159.2 mAh g <sup>-1</sup>	128.5 mAh g <sup>-1</sup>	120.3 mAh g <sup>-1</sup>	116.4 mAh g <sup>-1</sup> 1	This work

## References

- 1 Y. Tang, W. Li, P. Feng, M. Zhou, K. Wang, Y. Wang, K. Zaghbi and K. Jiang, *Adv. Funct. Mater.*, 2020, **30**, 1908754.
- 2 F. Peng, L. Yu, P. Gao, X.-Z. Liao, J. Wen, Y.-s. He, G. Tan, Y. Ren and Z.-F. Ma, *J. Mater. Chem. A*, 2019, **7**, 22248-22256.
- 3 Y. Shang, X. Li, J. Song, S. Huang, Z. Yang, Z. J. Xu and H. Y. Yang, *Chem*, 2020, **6**, 1804-1818.
- 4 Y. Mao, Y. Chen, J. Qin, C. Shi, E. Liu and N. Zhao, *Nano Energy*, 2019, **58**, 192-201.
- 5 W. Li, C. Han, W. Wang, Q. Xia, S. Chou, Q. Gu, B. Johannessen, H. Liu and S. Dou, *Adv. Energy Mater.*, 2020, **10**, 1903006.